Multiphoton Fragmentation of PAMAM G5-Capped Gold Nanoparticles Induced by Picosecond Laser Irradiation at 532 nm

ARTICLE *in* THE JOURNAL OF PHYSICAL CHEMISTRY C · SEPTEMBER 2007

Impact Factor: 4.77 · DOI: 10.1021/jp072611k

5 AUTHORS, INCLUDING:

Anna Giusti
Charité Universitätsmedizin Berlin
26 PUBLICATIONS **348** CITATIONS
SEE PROFILE

Emilia Giorgetti
Italian National Research Council
137 PUBLICATIONS **809** CITATIONS
SEE PROFILE

Simona Cristina Laza
Ecole Centrale Paris
8 PUBLICATIONS **74** CITATIONS
SEE PROFILE

Francesco Giammanco
Università di Pisa
116 PUBLICATIONS **636** CITATIONS
SEE PROFILE

Multiphoton Fragmentation of PAMAM G5-Capped Gold Nanoparticles Induced by Picosecond Laser Irradiation at 532 nm

Anna Giusti,[†] Emilia Giorgetti,*[,‡] Simona Laza,[£] Paolo Marsili,[£] and Francesco Giammanco[£]

INSTM and Department of Chemistry and Industrial Chemistry DCCI, Genova University, Via Dodecaneso 31, Genova, Italy, INSTM and Istituto dei Sistemi Complessi, Consiglio Nazionale delle Ricerche, Via Madonna del Piano 10, Sesto Fiorentino (Firenze), Italy, and Department of Physics "E. Fermi", Pisa University, Largo Bruno Pontecorvo 3, Pisa, Italy

Received: April 3, 2007; In Final Form: August 13, 2007

Fifth-generation ethylendiamine-core poly(amidoamine) (PAMAM G5)-capped gold nanoparticles were prepared by picosecond laser ablation in water, with the fundamental and second harmonic of a picosecond Nd:YAG laser. Although the visible wavelength exhibited a lower ablation threshold than that of the infrared one, the ablation process at 532 nm reached early saturation because of both linear and nonlinear absorption mechanisms, accompanied by fragmentation of existing nanoparticles. We demonstrate that the onset of the fragmentation can be monitored by simple UV−vis spectroscopy, thanks to the ability of PAMAM G5 to stabilize gold cations, which results in the growth of an intense band at 290 nm. We observed that, while with 532 nm (2.33 eV) irradiation a two-photon absorption mechanism induces fragmentation of the nanoparticles, the suspensions remain stable when irradiated with 1064 nm (1.17 eV) up to 60 GW/cm^2.

Introduction

Nanoparticles of noble metals are of great interest because of their potential applications to several rapidly developing fields, including tailor-made nanostructured materials for medicine and biosciences, drug delivery, in vivo cellular Raman spectroscopy[1,2] and, thanks to their characteristic plasmon resonances, for photonics and information technology.[3,4] In the case of gold, the nanoparticles (AuNPs) can be produced in the form of colloidal suspensions in solution either chemically[5] or physically by pulsed laser ablation of a metallic target, the second procedure being advantageous in terms of purity and biocompatibility of the final products.[6] Some studies have already been performed by using nanosecond and femtosecond pulses[7−9] and different stabilizing agents, such as sodium dodecyl sulfate (SDS) and thiols,[6] in order to prevent aggregation and subsequent precipitation of the nanoparticles.

Several authors have observed that, under certain wavelength and fluence conditions, metal nanoparticles can undergo a photofragmentation effect that, in the case of gold, takes place when irradiated at 532 nm, close to their plasmon resonance.[6,8] This effect can be exploited to control the size and shape of AuNPs obtained with different methods. In the case of nanosecond radiation, it was attributed to a photothermal process due to direct heating of AuNPs induced by high laser fluence.[8] With picosecond pulses, the photofragmentation mechanism is expected to be different. In the case of Ag nanoparticles, Kamat et al. interpreted the photofragmentation produced by picosecond radiation in resonance with the plasmon band in terms of electron ejection due to multiphoton absorption and subsequent charging and disintegration of the particles into smaller size products.[10]

Dendritic compounds, such as different generations of ethylendiamine-core poly(amidoamine) (PAMAM), have already been successfully used for the chemical preparation of metal−dendrimer nanocomposites. Due to the large number of available binding sites and inner cavities, they can act either as conventional stabilizers or as nanoreactors, thanks to the ability to encapsulate small metal clusters or metal ions.[11] This property, which opens the way to new interesting applications, such as selective nanocatalysts, nanocapsules, gene vectors, photon transductors, biosensors, and drug delivery systems, can also be advantageously exploited to investigate the production mechanism of the nanoparticles[12] and their photostability.

In this paper, we illustrate how, by using the fifth generation of PAMAM (PAMAM G5) as a stabilizer for gold nanoparticles obtained by picosecond laser ablation in water, it is possible to isolate charged metal clusters and attribute their origin to a multiphoton fragmentation process induced by the 532 nm laser wavelength.[6,8,10] The ability of PAMAM G5 to stabilize charged metal clusters makes it possible to visualize and monitor the onset of the photofragmentation by simple UV−vis spectroscopy of the suspensions.

Experimental Methods

We prepared AuNPs by focusing the fundamental (1064 nm) or second harmonic (532 nm) of a mode-locked Nd:YAG laser (EKSPLA PL2143A: rep. rate 10 Hz, pulse width 25 ps at 1064 nm and 20 ps at 532 nm) on a gold target. The experimental setup is sketched in Figure 1. The pulse energy was varied from 0.1 to 40 mJ and the ablation time from a few seconds to several hours. The focusing conditions of the laser beam were maintained constant in all of the experiments, and the diameter of the laser spot on the gold target was fixed at 1.4 mm with both wavelengths. The gold target (Goodfellow) was placed in a 1 cm × 1 cm quartz cuvette and was kept 2 cm in front of the focal plane of the laser beam. We used 2 mL of stabilizing solution, both for ablation and post-irradiation tests, and the liquid column above the target was 2 cm. The ablation process and the subsequent production of nanoparticles were monitored

[†] Genova University.
[‡] Consiglio Nazionale delle Ricerche.
[£] Pisa University.

10.1021/jp072611k CCC: $37.00
Published on Web 09/21/2007

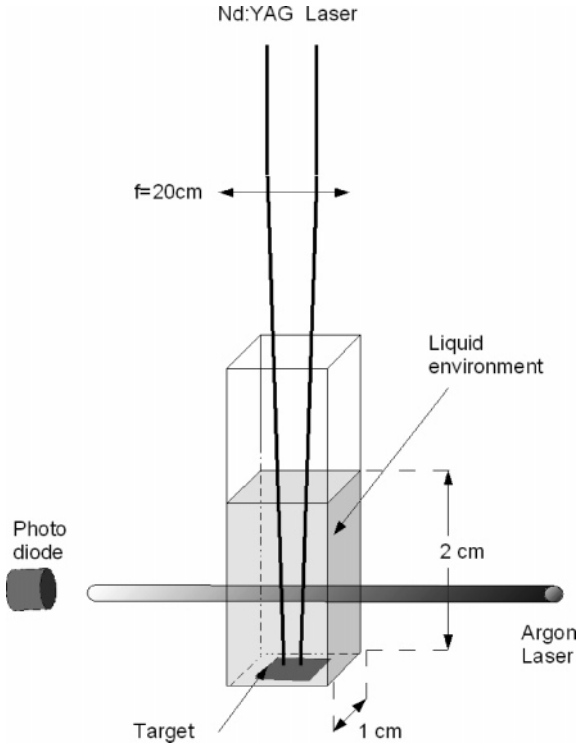

Figure 1. Schematic of the laser ablation setup; $f = 20$ cm is the focal length of the converging lens.

by measuring on-line the transmission T of a low-power beam at 514.5 nm from an Ar laser.

If not differently specified, we prepared AuNP suspensions in solutions of PAMAM G5 in water. The solutions were 3.8 mM, referred to superficial amino groups, and were obtained by dilution of a 22.2% aqueous solution of PAMAM G5 from Dendritech with ultrapure water (18.2 MΩ·cm at 25 °C). According to tabulated values provided by the producer, PAMAM G5 is a monodisperse compound, having a molecular diameter of 5.4 nm.

SDS was from Carlo Erba Reagents and dissolved in ultrapure water.

For the chemical synthesis of PAMAM-AuNPs suspensions, we followed the procedure described in ref 13. Aqueous solutions of PAMAM G5 were mixed with aqueous solutions of $HAuCl_4$ at controlled stoichiometries and stirred for 20 min. Subsequently, we added an excess of a freshly made ice-chilled sodium borohydride solution ($NaBH_4$) in 0.3 M NaOH and obtained the immediate formation of colloidal gold, indicated by a color change of the samples that turned red or brown.

We recorded UV−vis spectra with a double-beam spectrophotometer (Perkin-Elmer model Lambda19) 1 day after the preparation of the suspensions.

The particle mean diameter and dispersivity were determined by TEM analysis. TEM samples were obtained by dipping copper grids in the suspensions, and the images were recorded with a HRTEM JEOL2010, 200KV.

Experimental Results

The formation of gold nanoparticles having diameters larger than 1−2 nm can be monitored by UV−vis absorption spectra that typically exhibit a band around 520 nm, associated with plasma oscillations of conduction electrons within the gold particle (plasmon band, PB). The spectral position, shape, and width of the PB depend on the dimensions and polydispersivity

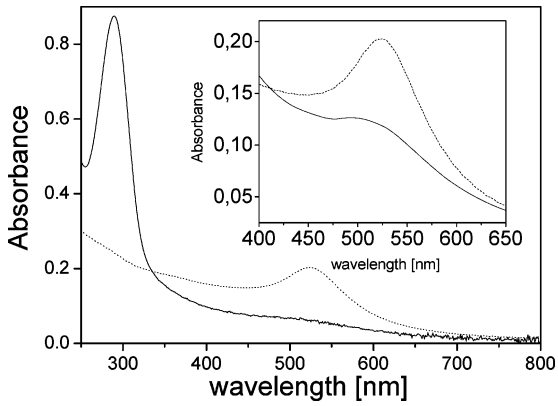

Figure 2. UV−vis absorption spectra of Au−PAMAM colloids obtained by laser ablation with 15 mJ pulses, 16 min at 532 (continuous lines) and 1064 nm (dotted lines). The optical path length (OPL) is 0.2 cm. The inset shows a magnification in the spectral region of the plasmon band. In the case of the 532 nm spectrum shown in the inset, we chose a longer OPL (1 cm) in order to better visualize the weak PB.

of the nanoparticles, on the dielectric properties of the surrounding medium, and on surface-adsorbed species.[14]

Figure 2 reports the absorption spectra of PAMAM G5 AuNP suspensions obtained with 532 and 1064 nm ablating wavelengths and 15 mJ of energy per pulse. In our experimental conditions and taking into account the 0.2 cm^{-1} absorption of the water column at 1064 nm, the fluence was 1 J/cm^2 for the visible beam and 0.7 J/cm^2 for the infrared beam. The figure includes an inset that magnifies the spectral region around the PB.

Figure 3 a,b reports typical TEM images and dimensional analysis of the suspensions of Figure 2. The samples were observed some days after the preparation. The particles are disaggregated and substantially spherical. The samples obtained with 1064 nm (Figure 3a) typically contain a small number of particles having a large diameter (more than 20 nm) and a large amount of smaller particles whose mean diameter and dispersivity are 3.5 and 1.5 nm, respectively. In the case of green-light ablation (Figure 3b), the particle mean diameter is (3.2 ± 0.7) nm, and there is no evidence of particles larger than 10 nm.

As shown in Figure 2, the biggest difference among the absorption spectra of the suspensions obtained with the two ablating wavelengths is in the UV region. The spectrum corresponding to 532 nm ablation exhibits an intense UV band peaked at 290 nm, which we never observed in the case of suspensions obtained with 1064 nm. This peak can be observed also in suspensions prepared with green light and a lower energy per pulse, as shown by the continuous line in Figure 4a, which was obtained by 532 nm ablation with 5 mJ pulses. It is related to the presence of the dendrimer, being absent in AuNP suspensions obtained with 532 nm in pure water, or aqueous solutions of other stabilizing agents, such as SDS (dotted line in Figure 4a). Moreover, it cannot be ascribed to photodegradation of PAMAM G5 molecules. This is demonstrated by the dashed curve in Figure 4a, which was obtained by 16 min green-light irradiation with 5 mJ per pulse of a 3.8 mM solution of PAMAM G5, in absence of the gold target. Indeed, the spectrum of the irradiated PAMAM G5 exhibits a small peak below 280 nm (see its magnification in the inset of Figure 4a). As reported in Figure 4b, this peak is a little more intense after laser irradiation (dotted and dashed lines), indicating that a certain amount of photodamage of the PAMAM G5 molecule cannot be excluded. As a matter of fact, a pronounced photodegradation mechanism is reported in ref 15, for the case of 254 nm

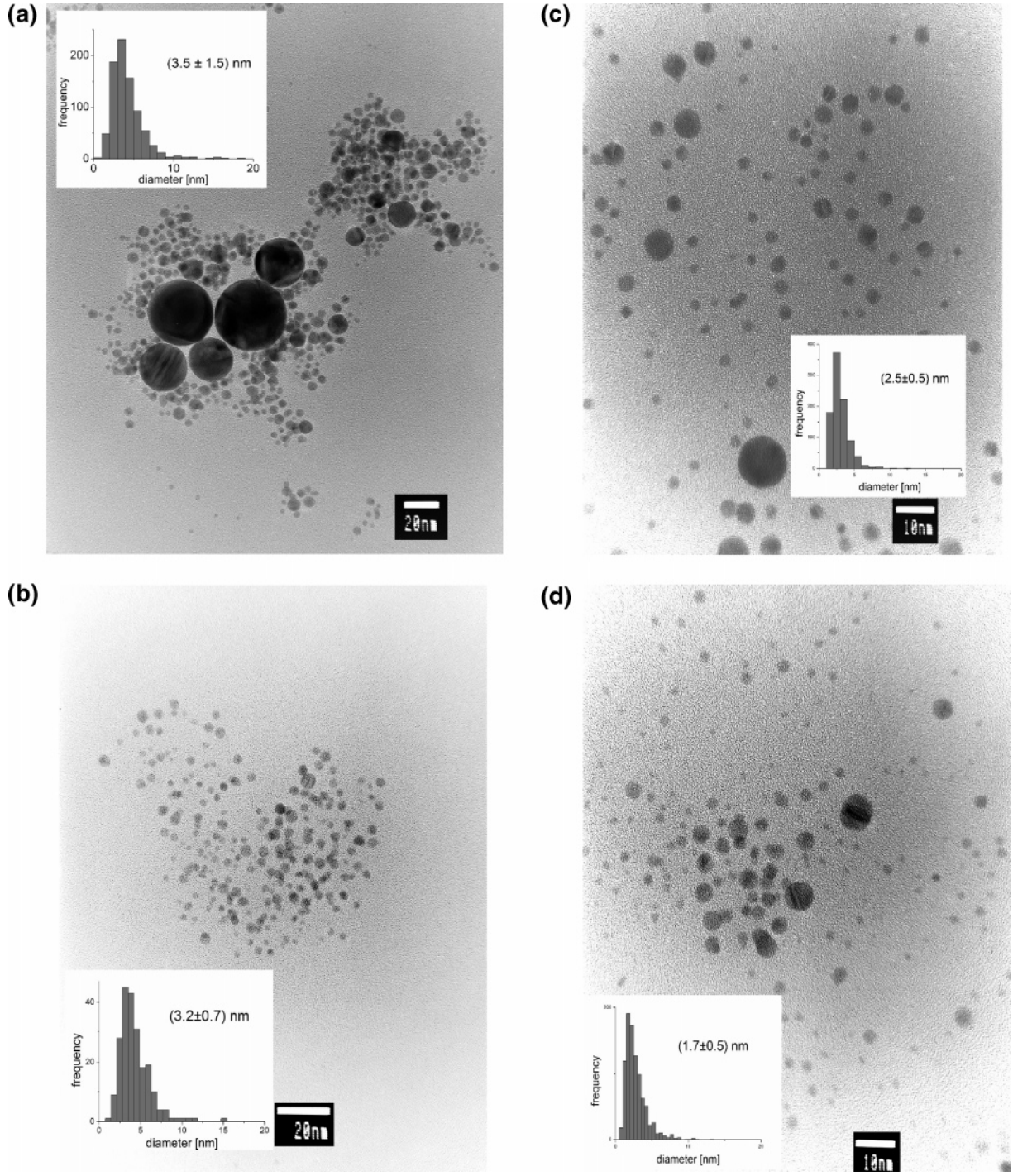

Figure 3. TEM analysis of gold dendrimer suspensions: (a) 1064 nm, 15 mJ, 16 min ablation; (b) 532 nm, 15 mJ, 16 min ablation; (c) suspension (a) after irradiation with 532 nm, 5 mJ, 16 min; (d) suspension (a) after irradiation with 532 nm, 10 mJ, 8 min.

irradiation of PAMAM G5 solutions with a mercury lamp. However, in our case, both the spectral position and the low intensity exclude that the small absorption below 280 nm can significantly contribute to the strong UV band observed in the presence of the Au target (continuous line in Figure 4a). Following ref 16, the band at 290 nm can be reasonably attributed to a ligand-to-metal charge transfer (LMCT). In particular, its spectral position is an indication of the presence of charged gold species in the suspension.[16,17]

In order to confirm the previous hypothesis and to gather information on the origin of the peak at 290 nm, we performed two experiments. First, we produced some suspensions of gold nanoparticles by chemical reduction of $HAuCl_4$ by $NaBH_4$ in NaOH and recorded the UV−vis spectra before and after the reduction. These spectra are shown in Figure 5. The peak at 290 nm, which is not present in that of the PAMAM solutions (continuous line in Figure 4b), is well evident in $HAuCl_4$ solutions (Figure 5a) and in $HAuCl_4$−PAMAM G5 solutions (Figure 5b), that is, in solutions containing Au in an oxidation state larger than 0 (note the different path lengths used for Figures 4b and 5). As evidenced in Figure 5a,b, its intensity grows with the concentration of gold. After the addition of $NaBH_4$, the peak at 290 nm disappears and is substituted by a shoulder at 280 nm (Figure 5c). At the same time, in Figure 5c, the formation of AuNPs is confirmed by the growth of the plasmon band in the green region of the spectrum.

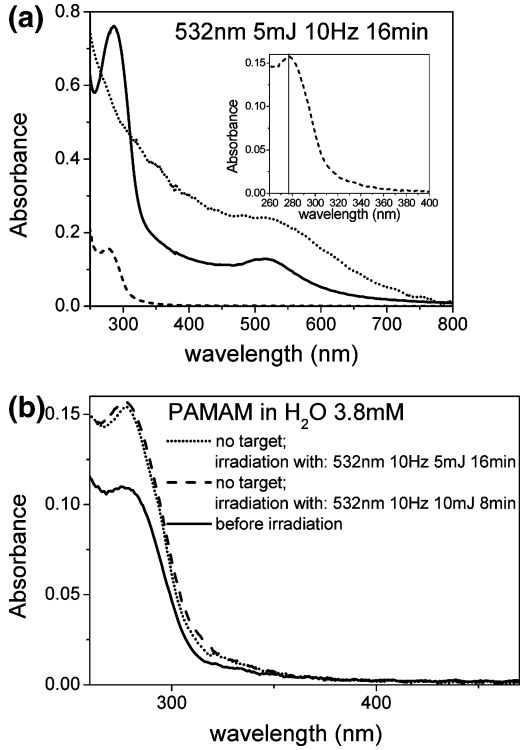

Figure 4. (a) UV−vis spectra of suspensions obtained by 16 min irradiation with 5 mJ pulses at 532 nm in the cases of PAMAM G5 in water without a gold target (dashed line), 0.1 M SDS in water with a gold target (dotted line), and PAMAM G5 in water with a gold target (continuous line). The inset is a magnification of the dashed-line curve. (b) UV−vis spectra of 3.8 mM solutions of PAMAM G5 in water before (continuous line) and after irradiation at 532 nm with 5 mJ pulses for 16 min (dotted line) and with 10 mJ pulses for 8 min (dashed line). (In order to better visualize the low absorbance of PAMAM G5 solutions, all of the spectra were obtained with OPL 1 cm.)

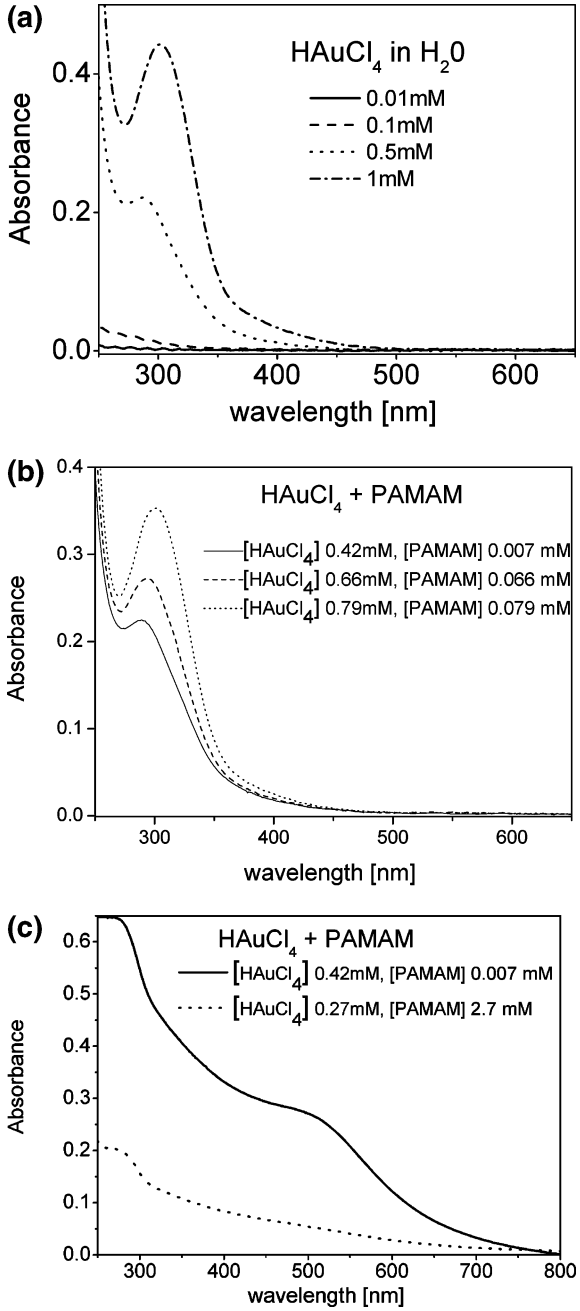

Figure 5. UV−vis absorption spectra of (a) $AuCl_4^-$ solution at different concentrations: 0.01 (solid line), 0.1 (dashed line), 0.5 (dotted line), and 1 mM (dash-dotted line); (b) PAMAM−$AuCl_4^-$ solutions at different molar ratios and concentrations: $[AuCl_4^-] = 0.42$ mM and [PAMAM] = 0.007 mM (solid line), $[AuCl_4^-] = 0.66$ mM and [PAMAM] = 0.066 mM (dashed line), $[AuCl_4^-] = 0.79$ mM and [PAMAM] = 0.079 mM (dotted line); (c) PAMAM−$AuCl_4^-$ solutions after reduction: $[AuCl_4^-] = 0.42$ mM and [PAMAM] = 0.007 mM (solid line), $[AuCl_4^-] = 0.27$ mM and [PAMAM] = 2.7 mM (dashed line). OPL 0.2 cm.

The second experiment was aimed at demonstrating that a similar reduction process can be obtained also in the case of suspensions produced by laser ablation of the gold target with 532 nm light. For this purpose, we added an excess of a freshly made ice-chilled $NaBH_4$ solution to a suspension obtained with 532 nm and 5 mJ per pulse. Indeed, as shown by Figure 6, the UV peak disappeared upon reduction, thus confirming the presence of charged species in the initial suspension. Actually, the reduction process took place only after the addition to the suspension of $NiCl_2$ powders that, in $NaBH_4$ solution, were reduced to Ni(0), which acts as a catalyst. The need of the catalyst suggests that at least a part of the positively charged gold clusters created by green light is located inside of the dendrimer,[16] and for this reason, they are less reactive than usual to $NaBH_4$. Note that in Figure 6 there is no significant change of the plasmon band since the reduction is expected to produce small neutral Au clusters that do not contribute to the plasmon resonance.

The 290 nm band can be also obtained by post-irradiating gold dendrimer suspensions without a target. Figure 7 illustrates the spectral changes of a sample obtained with 1064 nm (Figure 3a) and post-irradiated with the laser beam at 532 nm in two different conditions: 5 mJ, 16 min exposure (dashed line) and 10 mJ, 8 min exposure (dot-dashed line). After green-light irradiation, both spectra exhibited an intense peak at 290 nm and a partial bleaching of the plasmon band. In particular, it is worth noting that the energy dependence of the effect is nonlinear. Indeed, although the total amount of energy used in the two cases considered was the same (5 mJ × 16 min × 10 Hz = 10 mJ × 8 min × 10 Hz = 48 J), the process of plasmon photobleaching and subsequent growth of the band at 290 nm was more efficient with 10 mJ of energy per pulse. In contrast, as reported in Figure 4b, the small spectral change observed upon irradiation of AuNP-free solutions of PAMAM G5 does not depend on the energy of the single pulse. From these considerations, we infer that the most important difference when irradiating AuNP-free or AuNP-containing PAMAM G5 solutions is that (i) in the first case, the small photodegradation effect is linear, in the sense that it depends on the total amount of

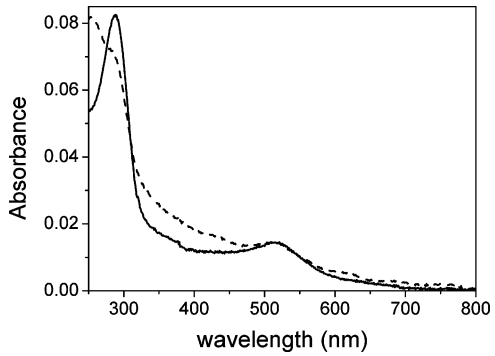

Figure 6. UV−vis spectra of gold dendrimer suspensions obtained by laser ablation with 5 mJ pulses and 532 nm, before (continuous line) and after (dashed line) chemical reduction obtained by adding an excess of a freshly made ice-chilled $NaBH_4$ solution. OPL 0.1 cm.

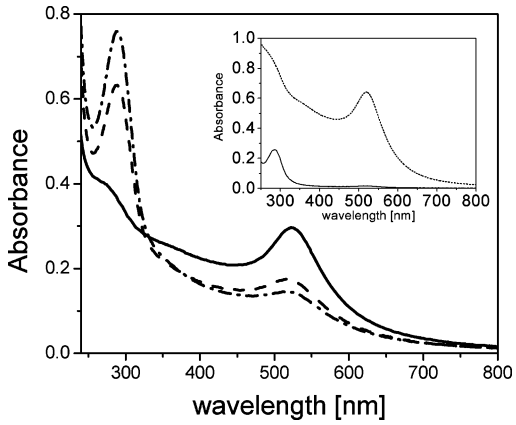

Figure 7. UV−vis spectra of a gold dendrimer suspension obtained with 15 mJ pulses at 1064 nm and 16 min, before irradiation (continuous line), after irradiation for 16 min with 5 mJ pulses at 532 nm (dashed line), and after irradiation for 8 min with 10 mJ pulses at 532 nm (dash-dotted line). In the inset are the UV−vis spectra of a suspension of AuNPs obtained with 15 mJ pulses at 1064 nm and 72 min, before (upper curve) and after (lower curve) irradiation for 4 h with 15 mJ pulses at 532 nm. Due to the presence of a large amount of precipitate, the irradiated sample was filtered with 1 μm pores. OPL 0.2 cm.

energy received by the sample (Figure 4b), and (ii) in the second case, the effect is strong and nonlinear, in the sense that the same amount of energy delivered by more energetic pulses results in a more efficient process (Figures 3c,d and 7).

The inset of Figure 7 shows that, after sufficient exposure, the plasmon band can be completely bleached. It refers to 4 h post-irradiation with 15 mJ of green light of a very concentrated suspension of AuNPs in PAMAM G5 obtained with 1064 nm, 15 mJ, and 72 min.

Figure 3c,d shows typical TEM images of the sample of Figure 3a after post-irradiation with picosecond pulses at 532 nm. In particular, Figure 3c corresponds to 16 min post-irradiation with 5 mJ pulses (dashed line in Figure 7) and Figure 3d to 8 min post-irradiation with 10 mJ pulses (dot-dashed line in Figure 7). Figure 3c,d demonstrates that the bleaching of the plasmon band illustrated in Figure 7 is accompanied by photofragmentation of existing AuNPs. The resulting mean particle diameter and dispersivity are (2.5 ± 0.5) and (1.7 ± 0.5) nm, respectively, with a considerable reduction of both parameters with respect to those from Figure 3a. The considerably larger reduction of particle diameter obtained with 10 mJ pulses is further proof of the nonlinearity of the photofragmentation process. After post-irradiation, the suspensions become more homogeneous, and the particle diameter seems to accumulate around the value of 1.7 nm. According to previous

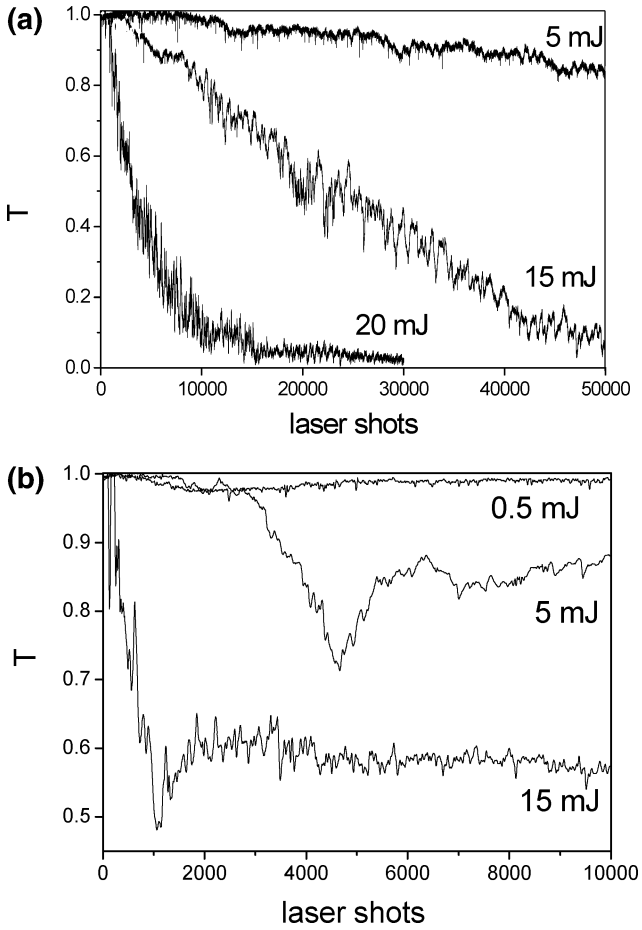

Figure 8. On-line transmission at 514.5 nm versus the number of laser shots for gold dendrimer suspensions obtained with 5, 15, and 20 mJ pulses at 1064 nm (a) and with 0.5, 5, and 15 mJ pulses at 532 nm (b). The beam at 514.5 nm crossed the cuvette 1 cm above the target.

studies on AuNPs obtained by chemical reduction and capped with PAMAM having different generations, this value is probably related to the dimensions of the inner cavities of our stabilizing molecule.[13]

In summary, (i) the 290 nm band does not appear in PAMAM-free suspensions (Figure 4), (ii) the dendrimer is not significantly damaged by laser irradiation with picosecond pulses at 532 nm (Figure 4b), (iii) the reduction process illustrated by Figure 6 demonstrates that 532 nm-irradiated samples contain charged gold species, and (iv) the onset of the 290 nm UV band corresponds to the onset of plasmon bleaching, accompanied by photofragmentation of AuNPs (Figures 3 and 7).

On the basis of the previous results, we conclude that the 532 nm beam produces Au^{3+} cations, isolated or associated to Au(0) colloids. The presence of gold cations is evidenced by the band at 290 nm, which can be considered a fingerprint of the process. In principle, their formation could be due either to direct ejection from the target,[18] to photofragmentation of existing AuNPs,[10] or to both mechanisms.

A deeper insight of the ablation process is obtained from the analysis of the on-line transmission T of the suspensions at 514.5 nm (that is very close to the PB) versus the number of laser shots. Figure 8 a,b reports these data obtained with different ablating wavelengths and energies.

In the case of 1064 nm, we recorded T(514.5 nm) for different values of energy per pulse, from 20 down to 5 mJ (Figure 8a). In particular, 5 mJ is the minimum energy that produced an appreciable decrease of T together with a buildup of the PB.

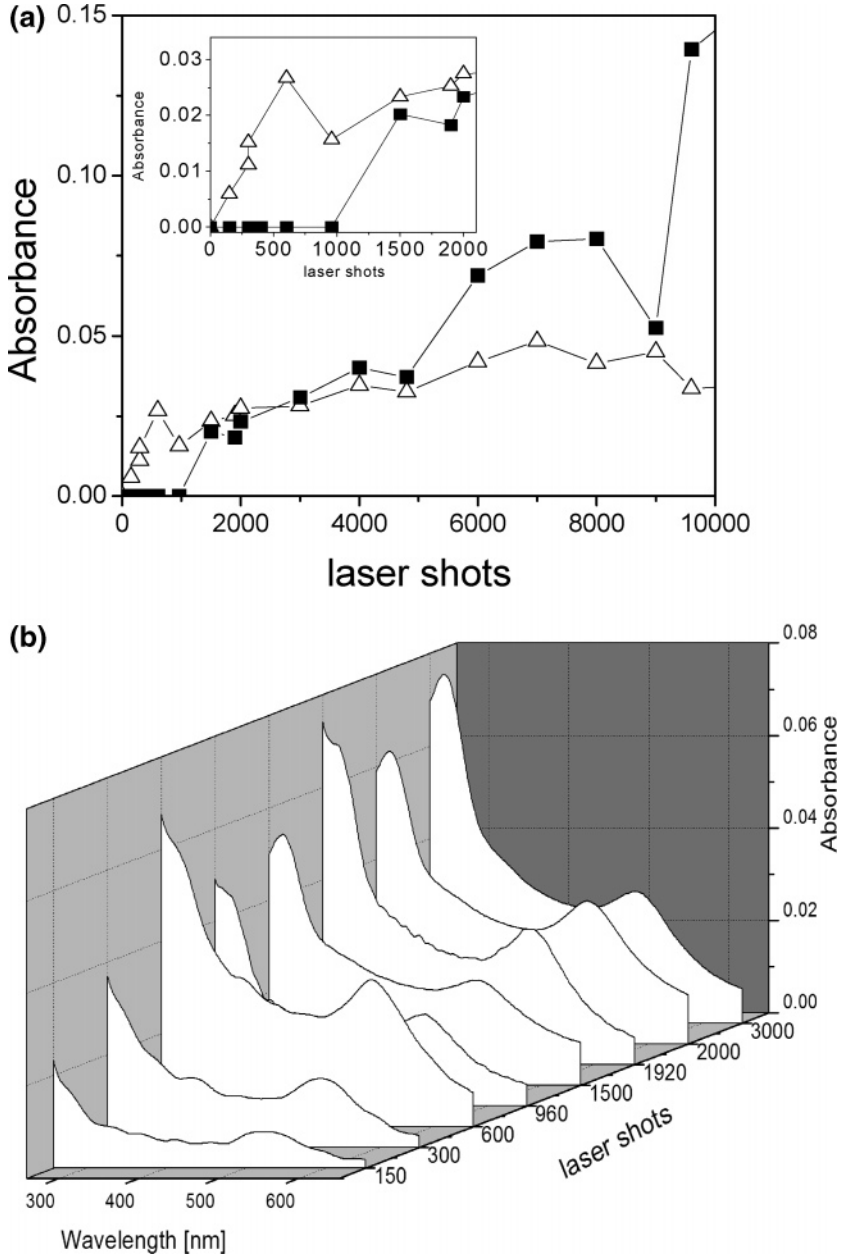

Figure 9. (a) Absorbance versus laser shots in the PB (triangles) and at 290 nm (squares). The inset shows a magnification of the initial part of the curves. (b) UV−vis spectra of AuNP suspensions obtained by different ablation times with 5 mJ pulses at 532 nm. OPL 0.2 cm.

All curves exhibit similar features; after an initial induction time, the transmittance decreases monotonically, and for sufficiently long exposure and energy, it reduces to 0. From these data, we can infer that the only process taking place with 1064 nm is the extraction of gold from the target, with subsequent and progressive growth of the concentration of nanoparticles.

In contrast, a more complicated behavior was observed with the 532 nm ablating wavelength, as reported by Figure 8b. The decrease of *T*, associated with the buildup of the plasmon band, started around 0.5 mJ. By examining in more detail the curve corresponding to the 5 mJ ablating energy, it is possible to distinguish a phase between 1 and about 1500 laser shots, where the transmittance is almost constant and which can be attributed to the nucleation of the particles. Instead, around 3000 shots, there was an abrupt decrement of *T* that can be associated to the growth of the dimensions of AuNPs and the consequent buildup of the plasmon band. Beyond 5000 laser shots, *T* increased and then saturated with an oscillatory behavior. This increase was caused by photofragmentation of existing AuNPs.[6,8,10] This interpretation is confirmed by Figure 9a, which reports the values of the absorption in the PB (triangles) and at 290 nm (squares) versus the number of laser shots. These values were obtained from UV−vis spectra and are related to the concentration of AuNPs and of charged metal clusters, respectively. For more clarity, Figure 9b illustrates the evolution of the UV−vis spectra of the suspensions of Figure 9a during the first 3000 laser shots. While the plasmon band appeared in the spectrum after about 150 laser shots and rapidly saturated, the peak at 290 nm was clearly visible only after 1000 laser shots and continued to grow even beyond 10000 laser shots. This behavior is further evidence that the production of aqueous suspensions of AuNPs by green-light picosecond laser ablation is the result of the competition among different processes: (i) ablation → nucleation → growth, (ii) linear absorption of the laser beam → reduction of the energy reaching the target → decrease of the ablation rate and subsequent saturation of the plasmon band, and (iii) absorption of the laser beam → fragmentation.

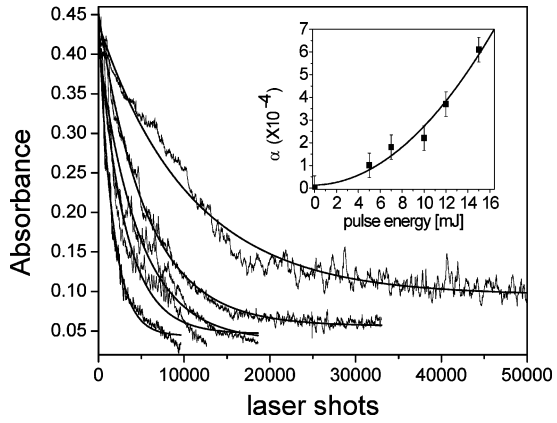

Figure 10. Effect of green-light exposure on the absorbance at 514.5 nm for a gold dendrimer suspension prepared with 1064 nm, 15 mJ, and 16 min and subsequently irradiated with 532 nm and 5, 7, 10, 12, and 15 mJ. The energy associated with each curve decreases in the upward direction of the figure. The inset shows the quadratic dependence of α versus the pulse energy. The beam at 514.5 nm crossed the cuvette 5 mm above the target.

The presence of PAMAM G5 molecules inhibits reaggregation of charged Au clusters and electrons and makes it possible to visualize and monitor the photofragmentation process by straightforward UV−vis spectroscopy.

In order to evaluate the energy dependence of the photofragmentation, we prepared a suspension with 1064 nm and monitored the on-line absorption at 514.5 nm during post-irradiation with 532 nm. The data were recorded for five different energies (5, 7, 10, 12, and 15 mJ per pulse) and are reported in Figure 10. The energy associated with each curve decreases in the upward direction of the figure. Due to the low diameter and dispersivity of our particles,[14] the absorbance at 514.5 nm and at time t, which is very close to the plasmon resonance, is approximately proportional to the concentration of AuNPs, $N(t)$. In this hypothesis, we can write that

$$\Delta N(t) = -N(t)\alpha\nu\Delta t \quad (1)$$

where ν is the laser repetition rate and α represents the probability that a nanoparticle, which is hit by the laser pulse, breaks into small fragments. In general, α depends on the energy of the laser pulse and provides a measure for the efficiency of the photofragmentation process. Simple integration of eq 1 gives an exponential decay for $N(t)$

$$N(t) = N_0 \exp[-\alpha\nu t] \quad (2)$$

where νt is the total number of laser shots. This simple scheme, which neglects the decay of the probe beam across the sample[19] and the effects of turbulence and diffusion, does not reproduce exactly the initial part of the curves and the step-like behavior that the absorbance exhibits in some cases. However, it can give useful indication on the order of the photofragmentation effect. For this purpose, we fitted the curves of Figure 10 with exponential functions and reported α versus pulse energy in the inset of Figure 10. This procedure returned a quadratic dependency of α on the energy, indicating that the fragmentation is the result of a two-photon absorption mechanism, which, following ref 10, leads to the ejection of conduction electrons and subsequent fragmentation of the particles. In contrast, no damage of the suspensions was observed after several hours of exposure to 1064 nm, up to 60 GW/cm^2. These data permit one to locate the work function of our PAMAM G5-capped AuNPs below 4.6 eV. Indeed, the work function of gold, which is 5.1 eV for the bulk, is expected to be much lower in the case of thin films or nanoparticles so that two photons at 532 nm can be sufficient to extract one electron from a AuNP.[20]

The parabolic fit of α versus pulse energy also contains a component that depends linearly on pulse energy and is 1 order of magnitude smaller than the quadratic one at low pulse energy. This component is probably associated with a thermal effect arising from the promotion of d electrons to the conduction band. Indeed, the laser frequency (2.33 eV) is strongly resonant with those states corresponding to the L point of the Brillouin zone of gold, for which the distance from the Fermi level is on the order of 2.4 eV.[21] A minor contribution to the linear term can arise also from the degradation of PAMAM G5, which follows a linear dependence on the laser energy (Figure 4b). However, the dominant effect is the two-photon coupling of the 532 nm laser beam with AuNPs.

Conclusions

We have demonstrated that the use of PAMAM G5 as the stabilizing agent of laser-produced AuNPs permits easy detection and monitoring of the concentration of charged metal species and consequent new insights both on the particle formation process and on their photostability. According to ref 10, the spectroscopic monitoring of such charged metal species is, in general, very difficult and effected by a large incertitude because of their weak contribution. The use of PAMAM overcomes this problem. In fact, the presence of charged metal species in the suspensions is made more visible by the onset of an intense charge-transfer band in the electronic spectra, centered at 290 nm. However, as evidenced in ref 17, different groups of the dendritic compound can be involved in the coordination of charged gold species. In our case, the available experimental data are not sufficient to identify the exact type of interaction. Moreover, at this stage, we cannot assert wether the gold cations are isolated in solution and coordinated by the dendrimer or if they are associated to some small Au(0) clusters.[16] These aspects deserve further experimental investigation.

We have shown that irradiation of AuNPs with intense picosecond pulses at 532 nm induces photofragmentation. Electron ejection followed by fragmentation of positively charged AuNPs seems the more likely mechanism in the presence of two-photon absorption. Part of the fragments, which can be either neutral or charged, recombine into smaller AuNPs, and part of them are stabilized by PAMAM G5 or trapped within its inner cavities. This effect can take place both during post-irradiation of AuNP suspensions and during the ablation process itself. The analysis of the 532 nm-induced photo fragmentation permits one to establish an upper limit to the work function of PAMAM G5-capped AuNPs, which is 0.5 eV lower than the value of 5.1 eV measured for bulk gold.

The photofragmentation of the particles and consequent growth of the band at 290 nm is never observed with 1064 nm, at least within the intensity range available in our experiments. Moreover, the absence of the charge-transfer band during ablation with 1064 nm suggests that, even if extraction of charged fragments from the target during the ablation process can, in principle, take place, such fragments coalesce into NPs on a time scale that is fast with respect to the laser repetition rate.

In conclusion, we stress that the detection of the 290 nm band and the monitoring of its temporal evolution can provide useful information not only on the mechanism of ablation and growth of AuNPs but also on their stability under light irradiation. In particular, while the plasmon resonance provides an indication

of the formation of neutral gold nanoparticles, the 290 nm charge-transfer band represents the fingerprint of the photofragmentation process.

Acknowledgment. The support by the Italian FIRB "Molecular and organic/inorganic hybrid structures for photonics" (Contract No. RBNE01P4JF) and by the CONACYT-CNR (Mexican−Italian) bilateral project "Synthesis and characterization of novel conjugated molecules for optical applications" is gratefully acknowledged. The authors wish also to thank Dr. C. Uliana of the Department of Chemistry and Industrial Chemistry of the University of Genova (Italy) for the TEM analysis of samples and Dr. F. Brandi of the Department of Physics of the University of Pisa (Italy) for useful discussions.

References and Notes

(1) Jain, P. K.; El-Sayed, I. H.; El-Sayed, M. A. *Nanotoday* **2007**, *2*, 18.

(2) Kneipp, J.; Kneipp, H.; McLaughlin, M.; Brown, D.; Kneipp, K. *Nano Lett.* **2006**, *6*, 2225.

(3) Alloisio, M.; DeMartini, A.; Cuniberti, C.; Petrillo, G.; Giorgetti, E.; Giusti, A.; Dellepiane, G. *J. Phys. Chem. C* **2007**, *111*, 345.

(4) Danckwerts, M.; Novotny, L *Phys. Rev. Lett.* **2007**, *98*, 26104.

(5) Daniel, M. C.; Astrucet, D. *Chem. Rev.* **2004**, *104*, 293.

(6) Mafunè, F.; Kohno, J.; Takeda, Y.; Kondow, T. *J. Phys. Chem. B* **2001**, *105*, 5114.

(7) Amendola, V.; Rizzi, G.; Polizzi, S.; Meneghetti, M. *J. Phys. Chem. B* **2005**, *109*, 23125.

(8) Amendola, V.; Polizzi, S.; Meneghetti, M. *J. Phys. Chem. B* **2006**, *110*, 7232.

(9) Kabashin, A. V.; Meunier, M. *J. Appl. Phys*. **2003**, *94*, 7941.

(10) Kamat, P. V.; Flumiani, M.; Hartland, G. V. *J. Phys. Chem. B* **1998**, *102*, 3123.

(11) Balogh, L.; Valluzzi, R.; Laverdure, K. S.; Gido, S. P.; Hagnauer, G. L.; Tomalia, D. A. *J. Nanopart. Res.* **1999**, *1*, 353.

(12) Giorgetti, E.; Giusti, A.; Laza, S. C.; Marsili, P.; Giammanco, F. *Physica Status Solidi C* **2007**, *204*, 1693.

(13) Groehn, F.; Bauer, B. J.; Akpalu, Y. A.; Jackson, C. L.; Amis, E. J. *Macromolecules* **2000**, *33*, 6042.

(14) Kreibig, U.; Vollmer, M. *Optical Properties of Metal Clusters*; Springer-Verlag: New York, 1995.

(15) Esumi, K.; Suzuki, A.; Aihara, N.; Usui, K.; Torigoe, K. *Langmuir* **1998**, *14*, 3157.

(16) Knecht, M. R.; Garcia-Martinez, J. C.; Crooks, R. M. *Langmuir* **2005**, *21*, 11981.

(17) Torigoe, K.; Suzuki, A.; Esumi, K. *J. Colloid Interface Sci.* **2001**, *241*, 346.

(18) Gibson, J. K. *J. Vac. Sci. Technol., A* **1998**, *16*, 653.

(19) Palchetti, L.; Qu, Li; Giorgetti, E.; Grando, D.; Sottini, S. *Appl. Opt*. **1997**, *36*, 1204.

(20) Tsang, T.; Srinivasan-Rao, T.; Fischer, J. *Phys. Rev. B* **1999**, *43*, 8870.

(21) Hache, F.; Ricard, D.; Flytzanis, C.; Kreibig, U. *Appl. Phys. A* **1988**, *47*, 347.